REPORT DOCUMENTATION PAGE

Form Approved
OMB No. 0704-0188

1. REPORT DATE *(DD-MM-YYYY)*	**2. REPORT TYPE**	**3. DATES COVERED** *(From - To)*
09 January 2017	Conference Paper	06 December 2016 - 11 January 2017

4. TITLE AND SUBTITLE
Computational Modeling of Supercritical and Transcritical Flows

5a. CONTRACT NUMBER

5b. GRANT NUMBER

5c. PROGRAM ELEMENT NUMBER

6. AUTHOR(S)
Harvazinski, M., Lacaze, G., Oefelein, J., Sardeshmukh, S., Sankaran, V.

5d. PROJECT NUMBER

5e. TASK NUMBER

5f. WORK UNIT NUMBER
Q1FZ

7. PERFORMING ORGANIZATION NAME(S) AND ADDRESS(ES) AND ADDRESS(ES)

Air Force Research Laboratory (AFMC)
AFRL/RQR
5 Pollux Drive
Edwards AFB, CA 93524-7048

8. PERFORMING ORGANIZATION REPORT NO.

9. SPONSORING / MONITORING AGENCY NAME(S) AND ADDRESS(ES)

Air Force Research Laboratory (AFMC)
AFRL/RQR
5 Pollux Drive
Edwards AFB, CA 93524-7048

10. SPONSOR/MONITOR'S ACRONYM(S)

11. SPONSOR/MONITOR'S REPORT NUMBER(S)
AFRL-RQ-ED-TP-2016-410

12. DISTRIBUTION / AVAILABILITY STATEMENT
Approved for Public Release; Distribution Unlimited. The U.S. Government is joint author of the work and has the right to use, modify, reproduce, release, perform, display, or disclose the work. PA Clearance Number: 16601; Clearance Date: 12/14/2016

13. SUPPLEMENTARY NOTES
For presentation at AIAA SciTech 2017; Grapevine, TX, USA; January 9-11, 2017
Prepared in collaboration with Sandia National Laboratories and Purdue University

14. ABSTRACT
Abstract: We examine the use of a single-fluid model with the Peng Robinson equation of state to model supercritical and transcritical flows with combustion. Both non-reacting and reacting flows are considered to understand the modeling challenges. Several modifications of the equations of state and mixture rules are tested and shown to have varying strengths and weaknesses. No method works uniformly well for both non reacting and reacting flows, although the use of the Peng-Robinson model with Amagat's mixture rule and modified compressibility factors appears to be robust and reasonably accurate for supercritical and transcritical combustion.

15. SUBJECT TERMS
N/A

16. SECURITY CLASSIFICATION OF:			**17. LIMITATION OF ABSTRACT**	**18. NUMBER OF PAGES**	**19a. NAME OF RESPONSIBLE PERSON**
					V. Sankaran
a. REPORT	**b. ABSTRACT**	**c. THIS PAGE**	SAR	21	**19b. TELEPHONE NO** *(include area code)*
Unclassified	**Unclassified**	**Unclassified**			N/A

Standard Form 298 (Rev. 8-98)
Prescribed by ANSI Std. 239.18

Computational Modeling of Supercritical and Transcritical Flows

Matthew E. Harvazinski,*
Air Force Research Laboratory, Edwards AFB, CA 93524, United States
Guilhem Lacaze,† Joseph Oefelein,‡
Sandia National Laboratories, Livermore, CA 94551, United States
Swanand Sardeshmukh,§
Purdue University, West Lafayette, IN 47907, United States
Venkateswaran Sankaran,¶
Air Force Research Laboratory, Edwards AFB, CA 93524, United States

Abstract: We examine the use of a single-fluid model with the Peng Robinson equation of state to model supercritical and transcritical flows with combustion. Both non-reacting and reacting flows are considered to understand the modeling challenges. Several modifications of the equations of state and mixture rules are tested and shown to have varying strengths and weaknesses. No method works uniformly well for both non reacting and reacting flows, although the use of the Peng-Robinson model with Amagat's mixture rule and modified compressibility factors appears to be robust and reasonably accurate for supercritical and transcritical combustion.

Nomenclature

a_m	Cubic parameter
A	Cubic parameter
b_m	Cubic parameter
B	Cubic parameter
k'_{ij}	Interaction parameter
p_c	Critical pressure
p_r	Reduced pressure (p/p_c)
T_c	Critical temperature
T_r	Reduced temperature (T/T_c)
V_m	Molar volume
X_i	Mole fraction of species i
Z	Compressibility
ω	Acentric factor

I. Introduction

Liquid rocket and gas turbine engines operate at high pressures. For gas turbines, the combustor pressure can be $60 - 100$ atm, while for rockets it exceeds 100 atm and can be as high as $300 - 500$ atm. Under these conditions, the propellants are typically injected at supercritical pressures, but are often at subcritical temperatures. The situation is further complicated since the propellants are injected into a mixture

*Research Aerospace Engineer, AFRL/RQRC, AIAA Member.
†Senior Member of the Technical Staff, AIAA Member
‡Distinguished Member of the Technical Staff, AIAA Senior Member
§Research Associate, AIAA Member
¶Senior Scientist, AFRL/RQ, AIAA Senior Member.

environment comprised of reactants and products. Whether or not the mixture is supercritical (i.e., above the vapor dome) is a function of the composition in addition to the local pressure and temperature. As a supercritical fluid is injected and mixes with the ambient fluid it may become locally subcritical even if the temperature and pressure remain constant. The subcritical and supercritical regions of the flow can have vastly different thermodynamic and transport properties, which can influence mixing and combustion dynamics in the combustor. Eventually, regardless of whether the reactants are in a subcritical or supercritical state, combustion occurs and the resulting high temperatures drive the system to a supercritical state. The existence of such a combination of states may be referred to as a transcritical state. Computational modeling of such phenomena is extremely challenging and is the subject of the current article.

A standard approach for supercritical flows is to treat the multicomponent mixture of species as a dense fluid using a real gas equation of state such as the Peng-Robinson cubic equation of state.[1] While the model is clearly valid for flows that are well above the vapor dome, their validity in the transcritical region, where one or more of the fluid components may drive the system to a saturated state, is not well established. The justification for the use of the dense-fluid approach is that the residence time is very short because of rapid mixing with the hot reaction products, which quickly pushes the mixture well above the vapor dome. The present work considers the numerical and physical modeling issues that arise when this "single-fluid" approach is used for representing transcritical flows under both non-reacting and reacting conditions.

Other more comphensive modeling options are certainly possible but they are much more involved. A homogenous two fluid model considers the vapor state and liquid state to be independent species. The species are assumed to be uniformly mixed and at the same temperature. There is no interface tracking or surface tension in this model.[2] In the case when surface tension becomes important, Eulerian-Lagrangian approaches that prescribe spray distributions and breakup can be used.[3] When empirically based atomization and breakup models are insufficient, a complete interface tracking method like the volume of fluid approach can be used. In such an approach the liquid gas interface is tracked.[4] We note that an overwhelming majority of the computational studies have similarly focused on purely supercritical flows, which serve to validate the use of different real gas equations of state, but fail to address the more complex transcritical regime.

Over the past decade, a substantial amount of work has been directed at studying the behavior of jets in transcritical environments. Chehroudi et al. collected visual images and jet spreading rates for jet injection into like and unlike ambient fluids for subcritical and supercritical conditions.[5,6] Leyva et al. have looked at supercritical nitrogen injection into a nitrogen environment under both unforced and acoustically forced conditions.[7] Roy et al. performed experimental work on the injection of supercritical jets into subcritical environments. Depending on the thermodynamic state they were able to produce results where surface tension became important and droplets were formed. Other conditions showed no droplet formation and behavior similar to supercritical/supercritical injection.[8] This indicates that this is an extremely complex operating state without clearly defined flow regimes.

Previous modeling work by Okong'o et al. focused on a supercritical binary mixing in a mixing layer. Using direct numerical simulation (DNS) they found that the strong density gradient hindered entrainment. Results also showed that the turbulent diffusion of species was more important than momentum.[9] Further work by Masi et al. on turbulent mixing layers developed effective locally varying turbulent Schmidt and Prandtl numbers which were observed to have negative values.[10] These two parameters can be used control the turbulent diffusion of mass and energy and have typically been assumed to be constant positive values in low-pressure environments.

In a comprehensive review article, Bellan cites two supercritical jet simulations and notes that a real gas equation of state along with unsteady simulations are the absolute minimum requirements for capturing supercritical behavior.[11] More recently, Zong et al. simulated supercritical N_2 injected into gaseous N_2 and found good agreement in the jet spreading angle with experimental data for two density ratios. We note that an overwhelming majority of the computational studies have similarly focused on purely supercritical flows, which serve to validate the use of different real gas equations of state, but fail to address the more complex transcritical regime. Oefelein simulated combustion between transcritical oxygen and supercritical hydrogen. It was found that intense property gradients were present that approached contact discontinuities which can be difficult to model.[12] Recently, Dahms and Oefelein have proposed a theoretical framework for assessing when a propellant mixture behaves as a supercritical dense fluid and when transcritical phenomena needs to be considered.[13] However, modeling of the transcritical regime remains a challenge.

As noted above, we evaluate the use of a single-fluid model based on the Peng Robinson equation of state under supercritical and transcritical conditions. Although our ultimate interest is in combustion, we

consider both non-reacting and reacting flows in order to understand the underlying modeling challenges. Under subcritical conditions, the intrinsic discontinuity present in the equation of state constitutes a physical and numerical inconsistency with the continuum assumption. For this reason, our objective is to modify the equation of state to remove the singularity and relax it to a continuous variation in thermodynamic phase space. Accordingly, the paper is organized as follows. In the next section, we summarize the Peng Robinson equation of state and present several modifications and smoothing treatments designed to keep the system of equations well-behaved. In addition, we consider different mixing rules in order to better control the mixture properties. We show that each of these methods have strengths and weaknesses. We consider results for both non-reacting and reacting jets. The non-reacting test cases are drawn from the experimental configurations of Cheroudi et al. that were mentioned erlier, while the reacting configuration corresponds to operating conditions and geometries relevant to liquid rocket engines. Based on these results, we provide several conclusions about the relative efficacy of employing single-fluid models for supercritical and transcritical problems.

II. Equation of State Model Adjustments

A. Peng Robinson Equation of State

A large number of cubic equations of state are available. A summary of the numerous different models is available in Poling et al.[14] The cubic equation of state used in the present work is the Peng-Robinson equation of state.[1] This is a three-parameter cubic equation of state which takes the form,

$$p = \frac{RT}{V_m - b_m} - \frac{a_m}{V_m^2 + 2b_m V_m - b_m^2} \tag{1}$$

The values of a_m and b_m can be found through a series of mixing rules. First, defining the values for an individual species i,

$$\kappa_i = 0.37464 + 1.54226\omega_i - 0.26992\omega_i^2 \tag{2}$$

$$a_i = 0.457235\frac{R^2 T_{c,i}^2}{p_{c,i}}\left(1 + \kappa_i(1 - \sqrt{T_r})\right)^2 \tag{3}$$

$$b_i = 0.077796\frac{RT_{c,i}}{p_{c,i}} \tag{4}$$

The parameters a_m and b_m are calculated through the following mixing rules using the values obtained for the individual species in the equations above,

$$a_m = \sum_{j=1}^{N}\sum_{i=1}^{N} X_i X_j \sqrt{a_i a_j} k'_{ij} \tag{5}$$

$$b_m = \sum_{i=1}^{N} X_i b_i \tag{6}$$

Here k'_{ij} is an interaction parameter which can be used to adjust the mixing rule for pairs of species, in most cases it is unity. Equation (1) can alternatively be written as a cubic equation, the roots of which are the compressibility Z,

$$Z^3 - (1 - B)Z^2 + (A - 2B - 3B^2)Z - (AB - B^2 - B^3) = 0 \tag{7}$$

where the compressibility is,

$$Z = \frac{pW}{\rho RT} \tag{8}$$

In the case of multiple positive real roots, the largest value of Z is typically selected. The parameters A and B depend on the mixture and are related to a_m and b_m through the following definitions,

$$A = a_m \frac{p}{R^2 T^2} \tag{9}$$

$$B = b_m \frac{p}{RT} \tag{10}$$

In addition to the above equations, departure functions are used to calculate all other thermodynamic properties.[14] Figure 1 shows the density of nitrogen calculated using the Peng Robinson equation of state for several reduced pressures. The model captures the high density at very low temperatures and the supercritical behavior at high reduced pressures. The model does not however provide a solution to the thermodynamic state inside the dome. Reduced pressures of 0.43, 0.63 and 0.83 show sharp transitions from the high density to the low-density regimes. The implication of the single fluid model is that near the transition point when the temperature shifts slightly the density (and other properties) will immediately jump in value. This presents a numerical challenge because small changes in temperature (e.g., less than 0.1 K) can result in order of magnitude changes in density and specific heat. Above a reduced pressure of 1.03 the transition between the high-density region and low-density region is smooth, but still exhibits non-ideal gas behavior. A similar plot can be generated for a multi-component mixture. The challenge with a mixture is that the transition region is also a function of composition in addition to the pressure and temperature. In a reacting flow computation avoiding this problematic transition region is impossible due to the wide varying properties of the mixture.

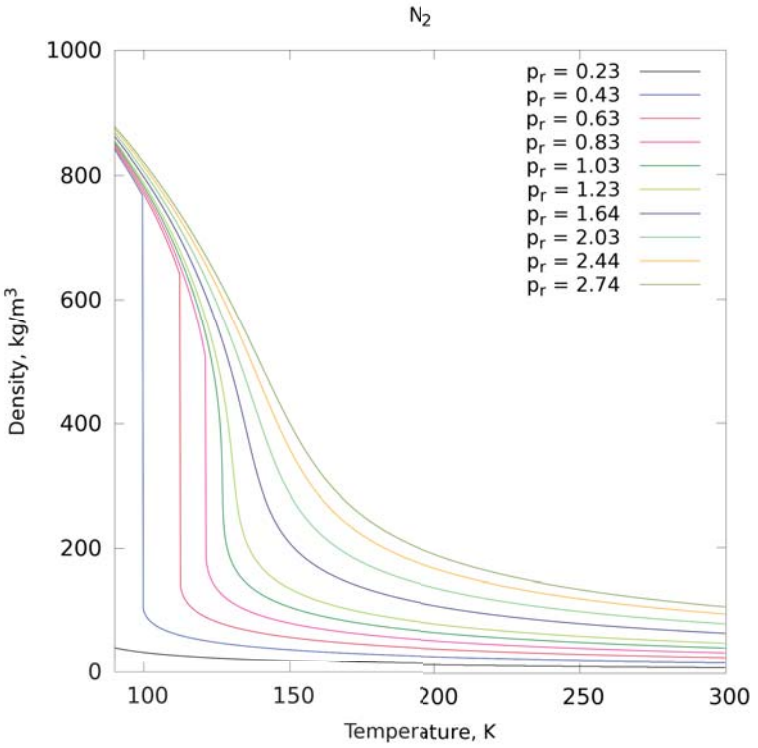

Figure 1: Density over the temperature range of interest. Each curve corresponds to a different reduced pressure.

B. Compressibility Smoothing

In addition to the sharp jump of density in the vapor dome at subcritical conditions (reduced pressure lower than unity), the use of a cubic equation of state in the context of a single fluid model leads to a discontinuity in other thermodynamic properties. Enthalpy and sound speed are no longer continuous and constant pressure specific heat tends to infinity. This results in numerical stiffness that cannot be handled properly by most of numerical methods currently used in computational fluid dynamics in the space propulsion community.

The initial proposed solution to improve the numerical stability while remaining with a single fluid model is to artificially smooth the transition region through the dome region. The argument being that in practice the exact behavior inside this region for injector type simulations is restricted to a very small region in the flowfield. Creating a method to traverse this region ensures that the simulation progresses in a stable fashion. In the dome region there will be three real roots to the cubic equation (Eq. 7). Let Z_i be the ordered roots

to Eq. 7 ordered such that,

$$Z_1 > Z_2 > Z_3 \tag{11}$$

Figure 2 shows a plot of the three roots in the region of interest for nitrogen at a reduced pressure of 0.63. The density is also shown for comparison. The compressibility used to define the density is always Z_1, which is $\max\{Z_i\}$. In the region near the discontinuity there are three roots present, the largest root corresponds to the vapor phase density and the smallest root corresponds to the liquid phase density. The middle root is without physical meaning. The temperature range over which the three roots are present is bounded by T_L on the low side and T_H on the high side.

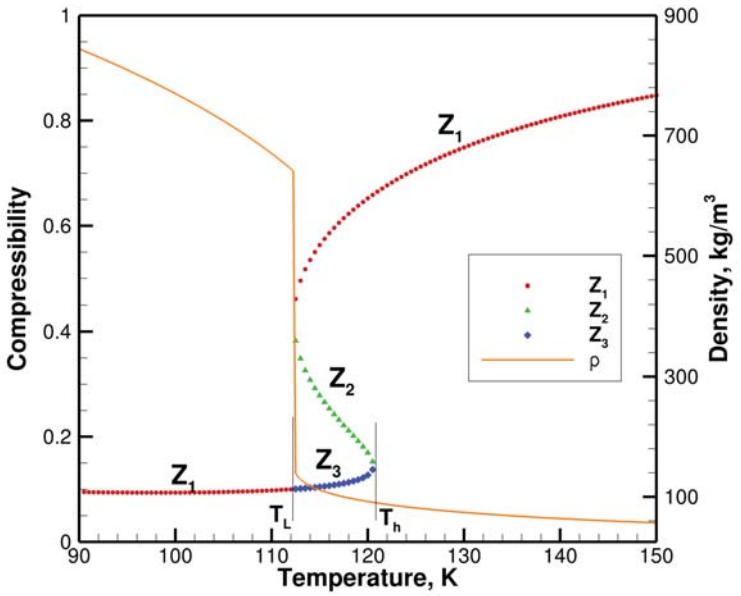

Figure 2: Roots to equation 7 along with density for nitrogen at a reduced pressure of 0.63.

In the current formulation, the compressibility is artificially smoothed through the transition region using the following definition of a "smooth" compressibility Z_s,

$$Z_s = Z_1 - \frac{Z_1 - Z_3}{2}\left[1 + \tanh G\right] \tag{12}$$

where the parameter G is,

$$G = a_g \left\{ \frac{p_{\max} Z_1 + Z_3}{1 + p_{\max}} - Z_1 + (Z_2 - Z_3) \right\} \tag{13}$$

Figure 3 shows the smooth root and the corresponding density. The thermodynamic derivatives of Z are also needed, and it was found that not applying the appropriate smoothing to derivatives of Z resulted in undesirable behavior of other thermodynamic quantities, especially at the interface where Z_s switches to Z_1. The derivative of the smooth root is,

$$Z_s' = Z_1' - \frac{1}{2}\left(Z_1' - Z_3'\right)\left(1 + \tanh G\right) + \left(Z_1 - Z_3\right) G' \tag{14}$$

$$G' = \frac{a_g}{\cosh^2 G}\left(Z_2' - Z_1' \frac{1}{p_{\max} + 1} - \frac{p_{\max}}{1 + p_{\max}} Z_3' \right) \tag{15}$$

The smooth density works very well for a single species. In the case of a mixture it was found that away from the dome region the smoothing could alter the solution. Figure 4 shows a mixture of 70% $C_{12}H_{26}$, 10% CO_2, 10% O_2 and 10% H_2 for a variety of pressures. Notice how in the two highest pressure cases at around 1300 K there is a spike in the density. A closer examination of solution to the cubic equation

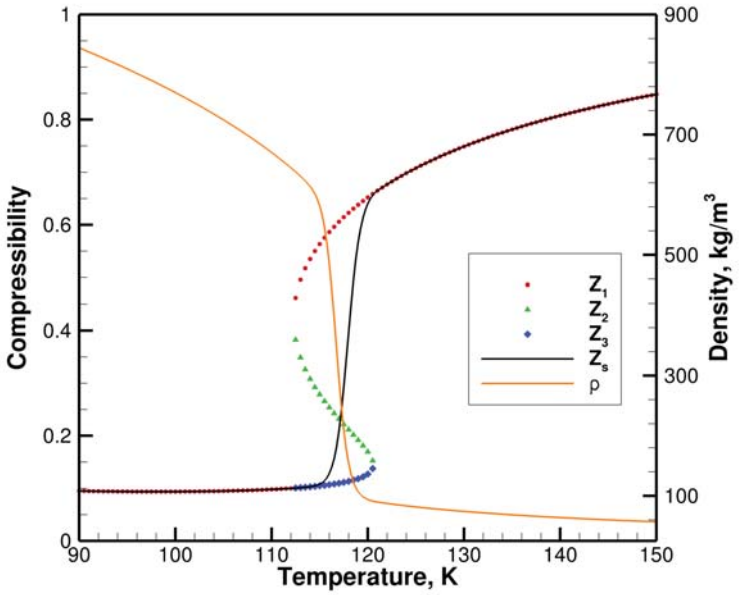

Figure 3: Roots to equation 7 along with the smooth root and the smoothed density for nitrogen at a reduced pressure of 0.63.

in this region reveals the presence of three real roots with at least one negative root. In order to improve the robustness of the smoothing and to allow it to be applied universally the criterion was modified to only apply the smoothing where all three real roots were found to be positive. Making this change restores the correct behavior of the high-pressure solutions at 1300 K, as shown in the figure.

The smoothing formulation introduces two new parameters, $p_{\max}$ and a_g. $p_{\max}$ controls the location of the smoothing and a_g controls the transition curvature. The smoothing is fairly insensitive to the parameter a_g and a value of 30 seems to provide adequate curvature at the transition points. Figure 5 shows the effect of $p_{\max}$ on pure nitrogen at a reduced pressure of 0.23. By tuning $p_{\max}$ the location of the transition is shifted. The smoothing alters other properties including the specific heat and sound speed. The expected behavior for the specific heat is to have a very sharp maximum at the critical temperature; this is instead shifted with the transition region, and the maximum specific heat shifts from being a near singular value to a broad peak with an overall maximum less than the unaltered solution. The sound speed should reach a local minimum at the critical temperature. In the case of the smoothing the minimum sound speed is further reduced and the transition occurs over a larger temperature range. The sound speed also exhibits some discontinuity where the compressibility shifts from Z_s to Z_1 at the high temperature point.

The difficulty with this smoothing is that it introduces unwanted changes to other thermodynamic properties like the specific heat and sound speed. Additionally, it is difficult to choose a single value of $p_{\max}$ that is suitable for a wide range of pressures. This is further complicated in the multi-species cases where the transition region is a function of temperature, pressure, and species composition. To address this several additional smoothing approaches were considered. The following sections briefly describe each approach. Following the descriptions a comparison of each of the methods is given. The problematic transition region where three real positive roots exist can be bounded by a lower temperature T_L and an upper temperature T_H. This range ΔT is the entire range there the three root system exists and was shown in Figure 2. The solution to a general cubic equation,

$$x^3 + ax^2 + bx + c = 0 \tag{16}$$

the discriminant determines the types of roots, real or complex, and is defined as,

$$\Delta = \frac{1}{2916}\left(2a^3 - 9ab + 27\right)^2 - \frac{1}{729}\left(a^2 + 3b\right)^3 \tag{17}$$

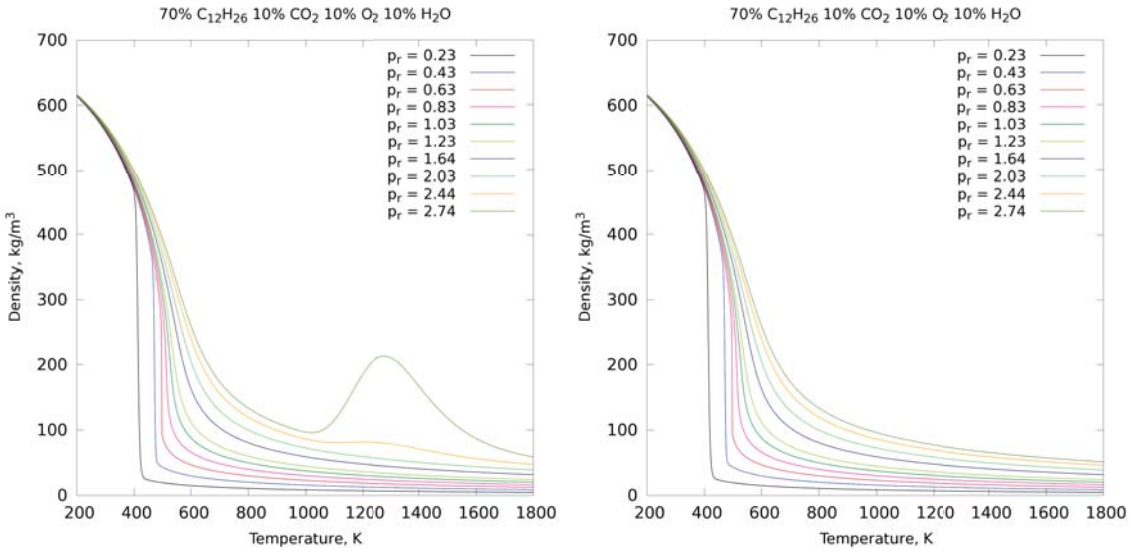

(a) Smoothing applied any time three real roots were found.

(b) Smoothing applied only when three positive real roots were found.

Figure 4: A negative real root can cause the smoothing operation to fail outside the dome region and alter the original solution.

The presence of three real roots occurs when the discriminant Δ is less than zero. To identify the temperature range under which the three real roots system is active the sign of the discriminant is examined. While varying temperature for a fixed pressure and mass composition the first temperature where the sign of the discriminant changes corresponds to T_L and where the discriminant changes sign again the temperature is T_H. Figure 6 shows the identification of the low and high temperatures based on the discriminant for nitrogen at a reduced pressure of 0.63.

1. Modified Hyperbolic Tangent Function

The first alternative method still uses a hyperbolic tangent to form the transition. At T_L and T_H the compressibility is a smooth function. In an effort to preserve the smooth property at these points which were shown to be problematic in the prior definition the smooth root is defined in terms of only the maximum Z_1 and the minimum Z_3 compressibility. The smooth compressibility is defined as,

$$Z_s = \frac{1}{2}\left[Z_1\left(1-\tanh\theta_s\right)+Z_3\left(1+\tanh\theta_s\right)\right] \tag{18}$$

where

$$\theta_s = 4\frac{T-T_c}{T_H-T_c} \tag{19}$$

and the center temperature T_c is,

$$T_c = \frac{T_L+T_H}{2} \tag{20}$$

2. Mirrored Z_2

The roots already form a continuous path between the minimum and maximum compressibility but it is not a one-to-one function. To exploit the continuous path, the root Z_2 must be mirrored so that Z is a function. The smooth root is defined as a piece-wise function of the three roots,

$$Z_s = \begin{cases} Z_1 & \frac{3\Delta T}{4} < T < T_H \\ \text{mirrored } Z_2 & \frac{\Delta T}{4} \leq T \leq \frac{3\Delta T}{4} \\ Z_3 & T_L < T < \frac{\Delta T}{4} \end{cases} \tag{21}$$

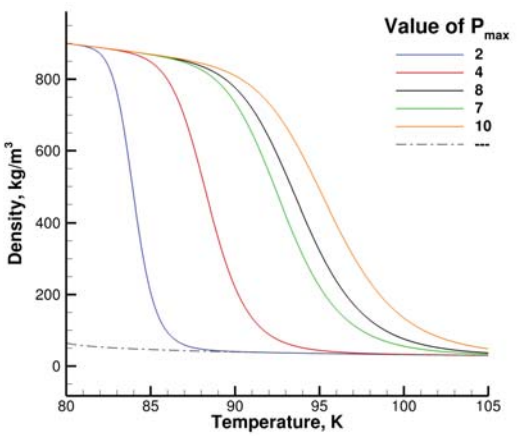

(a) Density.

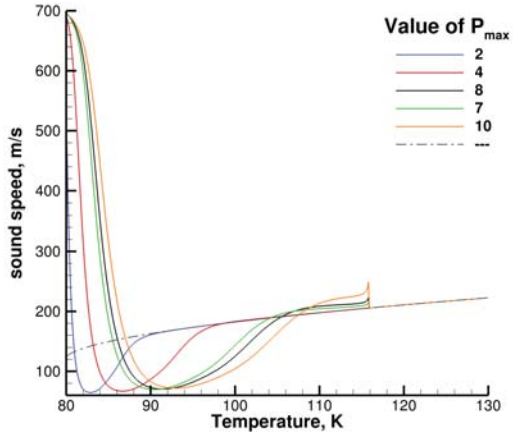

(b) Sound Speed.

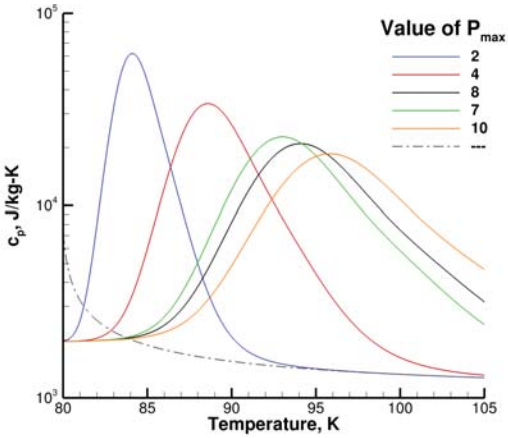

(c) Specific Heat.

Figure 5: The value of $p_{\max}$ is changed for pure N_2 at a reduced pressure of 0.23. In each case the black dashed line represents the original Peng Robinson solution.

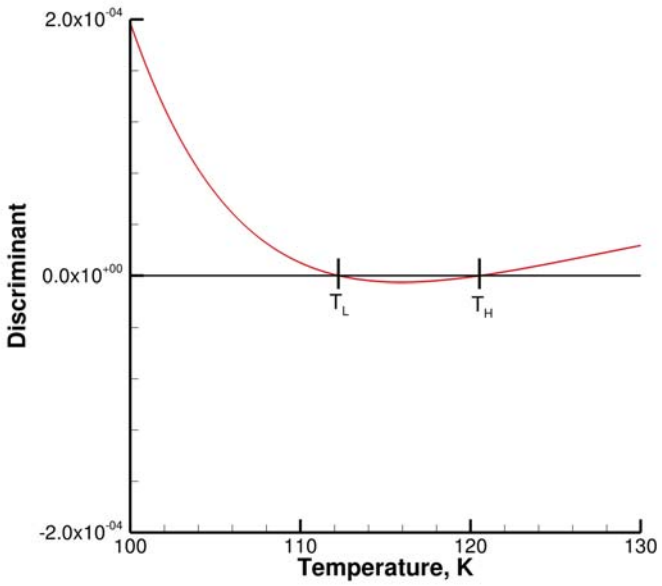

Figure 6: Variation of the discriminant of the cubic equation.

3. Cubic Polynomial of Temperature

Another straightforward way of approximating the compressibility is by obtaining a cubic fit between the compressibility at the lower and higher temperatures. To fit the coefficients of the cubic function $Z(T_L)$ and $Z(T_H)$ are used. Variations in temperature produce large changes in Z compared with pressure, and to account for this $\frac{\partial Z}{\partial T}\big|_{T_L}$ and $\frac{\partial Z}{\partial T}\big|_{T_H}$ are used as the additional equations to compute the coefficients of the cubic equation. The smooth root is then,

$$Z_s = a_1 + a_2 T + a_3 T^2 + a_4 T^3 \tag{22}$$

with the parameters obtained using the boundary conditions described above.

4. Using a Cosine Function

The analytic solution of the cubic equation in the region of interest requires determining a quantity θ. This θ can be shown to vary within the interval $\left[0, \frac{\pi}{3}\right]$. The earlier use of hyperbolic tangent requires the domain to be [-4,4] for obtaining [-1,1] range. Instead, the theta variation in this case can be exploited to formulate a smooth transition as,

$$Z_s = \frac{1}{2}\left[Z_3\left(1 + \cos 3\theta\right) + Z_1\left(1 - \cos 3\theta\right)\right] \tag{23}$$

The results of all of these approaches along with the original formulation have strengths and weaknesses in terms of specific properties. The difficulty is that there is not a clear "best choice" in smoothing the roots. Figure 7 shows a comparison of all proposed methods in determining the density, sound speed, and specific heat for $C_{12}H_{26}$ at a pressure of 1.8 MPa for a temperature range that spans the region of interest. Qualitatively the density is similar in each case, taking a slightly different path for each. The modified tanh and cosine approach have sharper transitions, especially at T_L. The sound speed variations show very different behavior from each other and from the original Peng Robinson solution. The cosine, cubic polynomial, and modified tanh approach cause the sound speed to increase in the transition region unlike the physical behavior. The original tanh and mirrored Z_2 method have a lower sound speed that is shifted away from the critical temperature. While the mirrored Z_2 method showed promise in the density and sound

speed it generates infinite values for the specific heat. That is because where Z_1 transitions to Z_2 and where Z_2 transitions to Z_3 the temperature derivative of compressibility is infinite. This effectively rules out this method. All of the other smoothing methods have a large band of high specific heats shifted away from the Peng Robinson value. Aside from eliminating the mirrored Z_2 method there is no clear best smoothing approach.

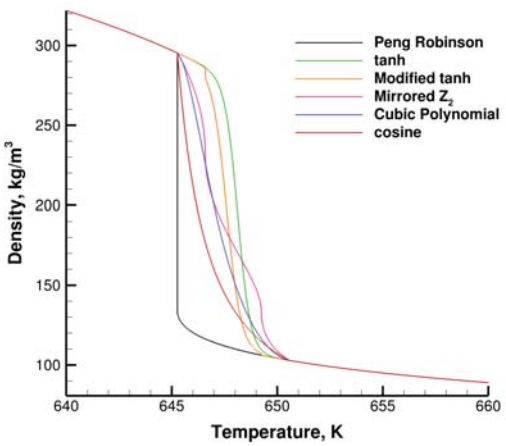

(a) Density.

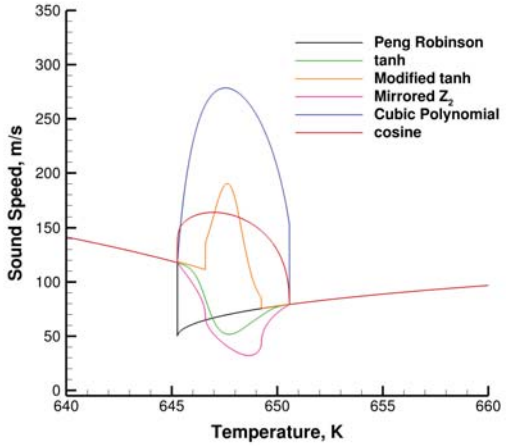

(b) Sound Speed.

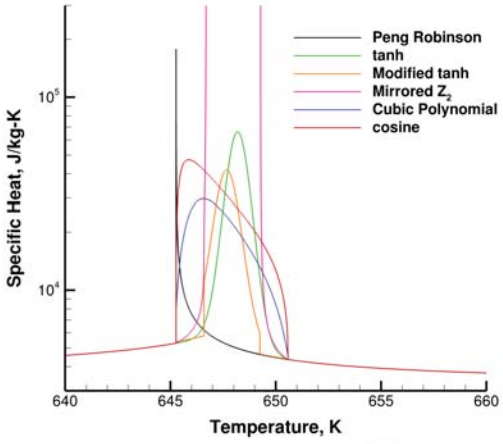

(c) Specific Heat.

Figure 7: The value of $p_{\max}$ is changed for pure N_2 at a reduced pressure of 0.23. In each case the black dashed line represents the original Peng Robinson solution.

C. Combining Peng Robinson with Amagat's Mixing Rule

The complex mixing rules associated with the principle of corresponding states results in problematic conditions when small amounts of water or carbon dioxide are added to cold fuel. This is a situation that will regularly occur in liquid rocket injectors where cold fuel slowly begins to burn and small amounts of water or carbon dioxide are present at lower temperatures. To help mitigate this a modified mixing rule based on Amagat's law has been implemented. In this approach, each species is treated individually as a real gas. This means that instead of a global compressibility, each species will have its own compressibility. In addition, departure functions for other properties are computed on a per-species basis as opposed to one departure function for the mixture. The following mixing rules are consistent with Amagat's law of partial

volumes. The mixture density is,

$$\rho = \left(\sum_{i=1}^{N} \frac{Y_i}{\rho_i} \right)^{-1} \tag{24}$$

where ρ_i is the partial density, defined as,

$$\rho_i = \frac{pW_i}{RTZ_i} \tag{25}$$

Other properties like enthalpy use the following mixing rule,

$$h = \sum_{i=1}^{N} \left(h_i + h_i^D \right) Y_i \tag{26}$$

Where h_i is the ideal gas enthalpy of species i and h_i^D is the enthalpy departure function for species i. Other properties like specific heat, entropy, and Gibbs energy are evaluated in the same manner. The mixtures compressibility can be defined as,

$$Z = \sum_{i=1}^{N} Z_i X_i \tag{27}$$

This approach yields a mixture compressibility that is similar to that found using the standard Peng Robinson model.[15] This model offers another potential advantage in controlling previously observed problematic behavior. Each species can be smoothed individually potentially removing the challenge in defining a universal smoothing parameter applicable to a disparate mixture. Figure 8 shows a comparison of a mixture of $C_{12}H_{26}$ with either water or carbon dioxide at 300 K for 3 MPa and 10 MPa. For water, there is very little difference in the computed densities for the two mixing rules. Carbon dioxide shows a significant departure at the lower pressure. This is because the range of $C_{12}H_{26}$ mass fractions spans the dome region.

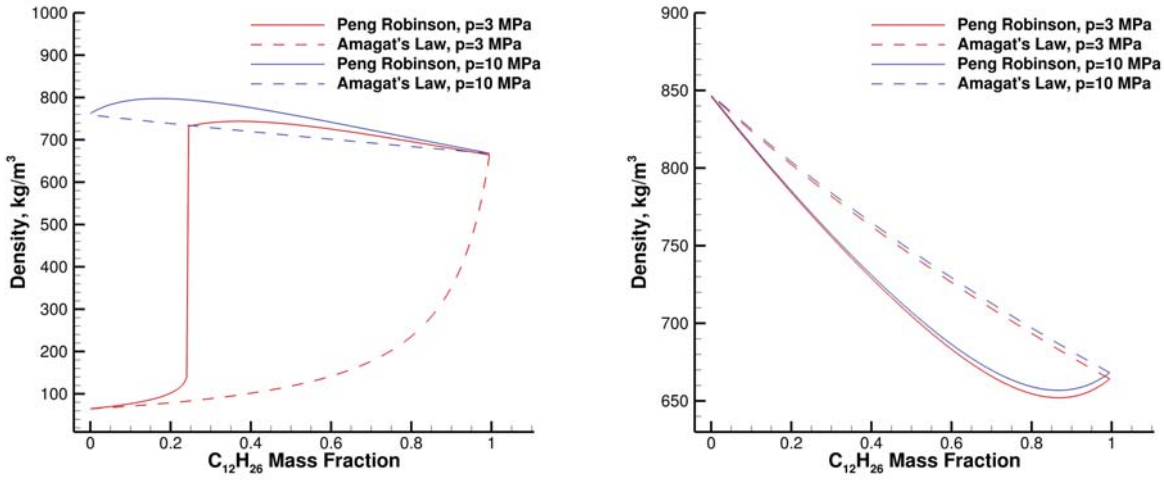

(a) $C_{12}H_{26}$ and CO_2 at 300 K.

(b) $C_{12}H_{26}$ and H_2O at 300 K.

Figure 8: The value of $p_{\max}$ is changed for pure N_2 at a reduced pressure of 0.23. In each case the black dashed line represents the original Peng Robinson solution.

D. Constant Compressibility for Reacting Shear Layers

Similar to the prior model in this case we have assumed that the real gas effects are limited to a very narrow region of the flowfield. The key issue with using an ideal gas model is that the density of the fuel (or oxidizer) will be too low. Since the mass flow rate is typically specified as the inlet boundary condition using the wrong inlet density will result in velocities that are incorrect. In this model a fixed value of $\bar{Z}$ is specified according to,

$$\bar{Z} = \frac{\rho_{rg}}{\rho_{ig}} \tag{28}$$

Here the real gas density, ρ_{rg}, is computed using the inlet boundary conditions from the Peng Robinon equation of state or a database like REFPROP. The mixing rule used in equation 24 is used. This model is more limited in that no real gas effects in the properties other than density are accounted for, and the value of $\bar{Z}$ is only accurate at the inlet conditions, as the fuel or oxidizer deviate from this operating point the approximation will worsen. In the configurations of interest however the fuel occupies only a small region and is typically quickly consumed. Figure 9 shows a comparison of the compressibility computed with Peng Robinson and the constant compressibility supplied at 300 K and 600 K.

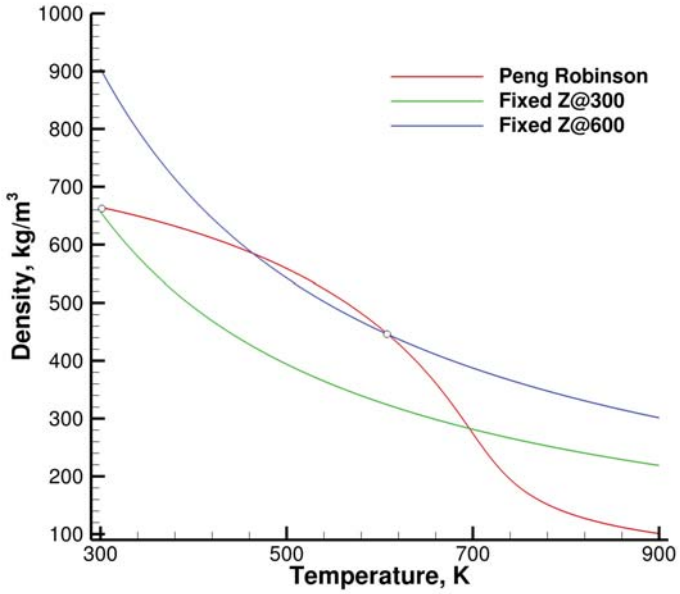

Figure 9: Comparision of the compressibility computed with Peng Robinson and the constant compressibility supplied at 300 K and 600 K.

Based on the figure it is clear that this approximation is only valid when the fuel remains close to the injection temperature where the compressibility was defined. Because the ideal gas curve does not match the real gas curve a simple multiplication of the compressibility has limited validity outside the region where it was defined. In a liquid rocket injector, we expect that the fuel is quickly burned and is present only in a small portion of the flowfield thus an such approximation may be acceptable. Importantly, the combustion products are a a higher temperature wherein the ideal gas assumption is usually valid.

III. Non-reacting Results

The simulations for the non-reacting case follow the work of Chehroudi et al. who performed a series of experiments primarily using nitrogen. Cold N_2 ($90 - 110\,K$) is injected into a chamber filled with warm N_2 ($300\,K$). This was done for a series of pressures where the reduced pressure ranged from 0.23 to 2.74. This spans the subcritical to supercritical pressure states. In doing so, they recorded vastly different injection behavior. At the low reduced pressure the jet is liquid like with surface instabilities. Above a reduced pressure of unity there is no breakup into droplets, instead there is a mixing layer with large density uniformities. At the highest reduced pressure the jet resembles a single phase turbulent jet.[6]

A representative two-dimensional planar geometry was created to examine the applicability of the smoothing to capture the subcritical to supercritical pressure states. A 5.5 mm by 0.4064 mm domain uses a uniform 256×512 Cartesian grid. The code is fifth order accurate in space and a third order explicit RungeKutta scheme is used for the time discretization. The simulations are run without a turbulence model. Nitrogen at 90 K is injected through a height of 0.127 mm at a velocity of 12.5 m/s. The remainder of the left boundary flows nitrogen at 300 K with a velocity of 0.5 m/s. Simulations were attempted using the tanh smoothing with the parameter $a_g = 30$ and $p_{\max} = 4.0$ for reduced pressures of 0.43, 0.63, 0.83, 1.03, 1.26, 1.64, 2.03, 2.44, and 2.74. All simulations with a reduced pressure of 1.03 or less failed to generate a stable solution that lasted through a single flow through time. Simulations with a reduced pressure of 1.26 and above were stable.

Figure 10 shows density contours for the reduced pressure of 1.64 and Figure 11 shows density contours for the reduced pressure of 2.74. Both simulations show a clear demarcation between the warm and cold nitrogen. The interface between the two fluid streams is characterized by a Kelvin Helmholtz type instability. In the case of the reduced pressure of 1.64 the roll-up is larger and starts closer to the inlet boundary compared with the reduced pressure of 2.74. Experimentally for the jet it was reported that above a reduced pressure of 2.04 there was a reduction in the core length and by 2.74 it visually looked like gas-gas mixing. The shear layer test case makes it difficult to draw conclusions about the core length but the results do visually look like gas-gas mixing.

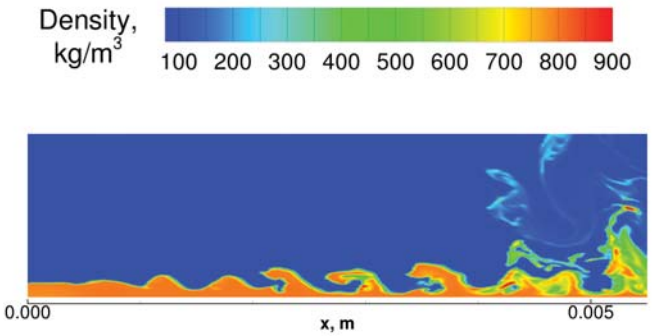

(a) Time 1.

(b) Time 2.

(c) Time 3.

(d) Time 4.

(e) Time 5.

Figure 10: Density plots for a reduced pressure of 1.64.

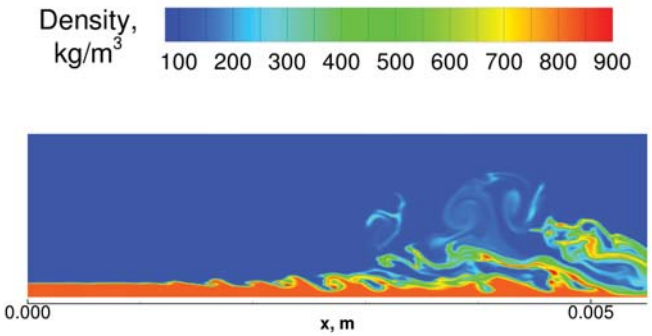

(a) Time 1.

(b) Time 2.

(c) Time 3.

(d) Time 4.

(e) Time 5.

Figure 11: Density plots for a reduced pressure of 2.74.

IV. Reacting Results

A two-dimensional shear layer representative of a $C_{12}H_{26}$ injector is used to test the constant compressibility ideal gas model. For this simulation, a code which is second order accurate in time and space is used. The mesh contains approximately 250,000 cells and has uniform spacing. The fuel is $C_{12}H_{26}$ and is injected at 600 K with a mass flow rate of $74.085\,\mathrm{kg/s \cdot m}$, the oxidizer is pure O_2 and is injected at 611 K with a mass flow rate of $145.3567\,\mathrm{kg/s \cdot m}$. The mean pressure is 3.846 MPa. For the fuel, these conditions are supercritical in pressure but subcritical in temperature. For the oxidizer, the conditions are subcritical in pressure and supercritical in temperature. A temperature of 600 K was chosen for the fuel because under simplified conditions without acoustic waves this case can be successfully run using the Peng Robinson model with tanh smoothing ($a_g = 30$ and $p_{\max} = 4.0$). The actual configuration is subjected to hydrodynamic and combustion instabilities and thus generates wide ranging pressure fluctuations that are not currently numerically stable with the Peng Robinson model. A simplified two step reaction mechanism is used.

Results from the two simulations are showing in Figures 12–14. The figures show the density, fuel mass fraction, and temperature. From the density plot it is clear that the fixed compressibility has difficulty maintaining a near uniform incoming density. Looking at different time snapshots of the density (not shown) shows that the density varies unlike the real gas approach which shows the same density at both times. This is likely because of pressure oscillations and the fact that the ideal gas equation of state with a fixed compressibility does not follow the same density curve as the real gas as the temperature and pressure change from the evaluation point of Z. Both simulations start burning at slightly different times so it is difficult to compare direct snapshots.

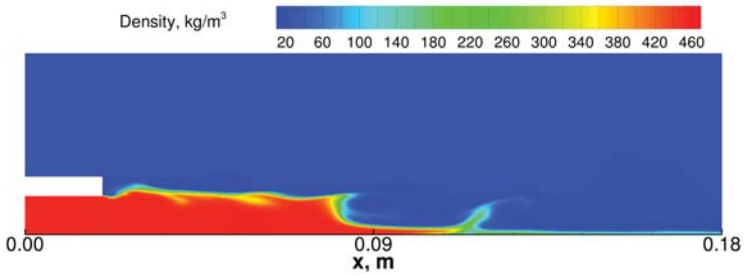

(a) Peng Robinson.

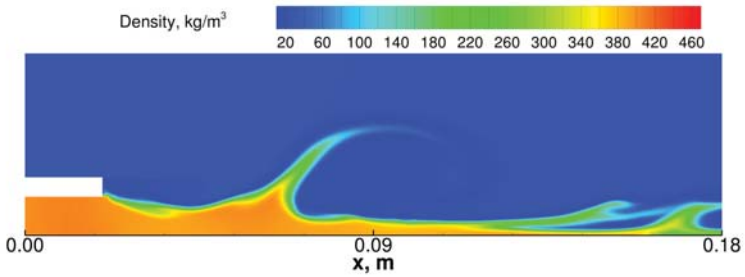

(b) Constant Z.

Figure 12: Density plots for the reacting shearlayer test case.

The fuel mass fraction along with the density identify differences in how the shear layer interface behaves for the two models. One difference is the sharpness of the interface between the fuel and oxygen. The real gas shows a steep gradient between the two while the density gradients are smoothed out in the other case. This is a result of the equation of state and should be further considered in evaluating the applicability of this model and how it affects the mixing of the propellants. There is also large scale roll up present in the fixed compressibility case that is not observed in the real gas simulation. Another difference is that as the fuel heats up (downstream) the density is significantly lower for the real gas equation of state. This is to be expected based on Figure 9, which showed that the density would be over predicted based on evaluating the compressibility at 600 K. A piecewise construction of Z at multiple temperatures may be able to better capture the behavior

Despite these differences the temperature plot shows a qualitatively similar combustion with a thin flame

along the interface between the fuel and oxygen. The flame is attached in both cases and is anchored to the splitting plate. This model is an attractive engineering model, especially when the computed value of Z is close to unity. But there are indications that under some conditions it may introduce significant differences from the real gas equation of state. A full understanding of how the fuel behaves and the length of time it remains in the combustor are key questions to answer before deciding if this model is applicable to a particular configuration.

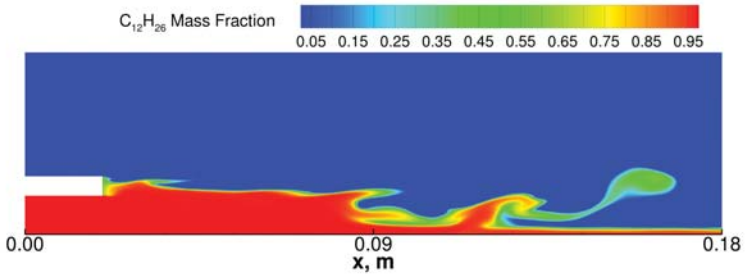

(a) Peng Robinson.

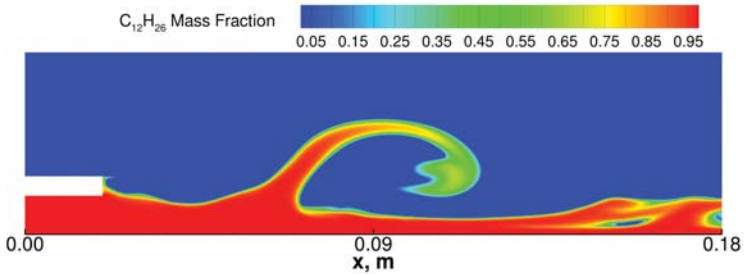

(b) Constant Z.

Figure 13: $C_{12}H_{26}$ mass fraction plots for the reacting shearlayer test case.

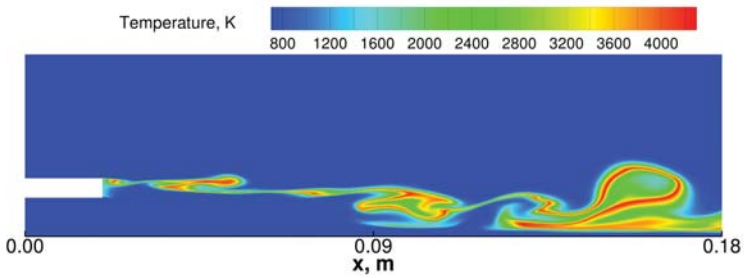

(a) Peng Robinson.

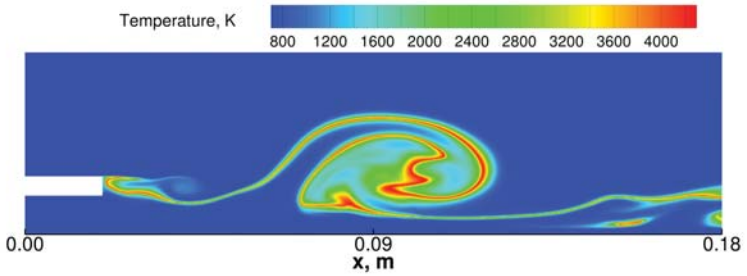

(b) Constant Z.

Figure 14: Temperature plots for the reacting shearlayer test case.

V. Conclusions

A series of smoothing options were presented to enable the Peng Robinson equation of state to perform without introducing numerically destablizing jumps in properties in the transcritical regime. The motivation was to enable a single fluid model for applications in liquid rocket injectors where the transcritical regime is restricted to a small local region inside the injector cup where the fuel and oxidizer initially begin to burn. The smoothing proved to be difficult and focused on the computation of the compressibility in the vapor dome. While it was simple to generate a density that had unique values for temperature and pressure, other thermodynamic quantities were problematic. Both the constant pressure specific heat and the sound speed have unique behavior near the critical point. The sound speed reaches a local minimum and the specific heat takes on extremely large values over a very narrow range. The smoothing was unable to fully capture that behavior despite multiple different approaches to generate a smooth compressibility.

A non-reacting nitrogen shear layer was tested for a range of reduced pressures using hyperbolic tangent smoothing that provided the best overall behavior. It was found that only simulations above the vapor dome (i.e., in the compressed liquid regime) were able to run successfully. Simulations which were sub-critical in pressure were numerically unstable. This may indicate that the single fluid approach to modeling this regime is inadequate and a Eulerian-Lagrangian or VOF approach is needed. It may also be a result of inadequate numerical stability to handle the extremely large thermodynamic gradients that are present. This will be considered in future work. Another issue is that the smoothing introduces inconsistencies, the value of Z is not consistent with a_m and b_m in the smoothing region. Since all three of these are used to compute other thermodynamic quantities it may be necessary to consistently recompute a_m and b_m. This is not straightforward and will also be considered in future studies.

While the non-reacting case is interesting, a major motivation of this work is the configuration with combustion. In some regards, this appears to be a simpler problem. As the flowfield reacts, the increase in temperature naturally moves it away from the vapor dome. The challenge for the reacting flow case is the introduction of water and carbon dioxide, which because of their high critical pressure, tend to shift mixtures toward the vapor dome. This can create local regions with vastly different properties, including sound speeds so low that the flow becomes locally supersonic. Two additional equation of state modifications were identified for this type of simulation. A modified mixing rule which used Amagat's law and a fixed compressibility. Both of these approaches exploit the fact that the real gas behavior is restricted to the incoming propellants and, for a short portion of time over a limited area, when the propellants mix. The majority of the flowfield where combustion has taken place will behave more like an ideal gas. The fixed compressibility case was compared with a smooth Peng Robinson case in a reacting shear layer configuration. The results showed qualitatively similar burning. There were differences in the computed density the Peng Robinson equation of state produced a near uniform density of the incoming fuel while the fixed compressibility showed variability because of local pressure fluctuations. Further work is needed to understand how to better control this, possibly by moving to the modified mixing rule.

References

[1]Peng, D. and Robinson, D., "A New Two-Constant Equation of State," *Industrial and Engineering Chemistgry: Fundamentals*, Vol. 15, 1976, pp. 59–64.

[2]Li, D., Sankaran, V., Lindau, J., and Merkle, C., "A Unfied Computational Formulation for Multi-Component and Multi-Phase Flows," *43rd AIAA Aerospace Sciences Meeting*, Reno, NV, January 2005.

[3]Reitz, R., "Modeling Atomization Processes in High-pressure Vaporizing Sprays," *Atomization and Spray Technology*, Vol. 3, 1987, pp. 309–337.

[4]Hirt, C. and Nichols, B., "Volume of fluid (VOF) method for the dynamics of free boundaries," *Journal of Computational Physics*, Vol. 39, No. 1, 1981, pp. 201–225.

[5]Chehroudi, B., Talley, D., and Coy, E., "Initial Growth Rate and Visual Characteristics of a Round Jet Into a Sub- to Supercritical Enviroment of Relevance to Rocket, Gas Turbine, and Diesel Engines," *37th AIAA Aerospace Sciences Meeting*, Reno, NV, January 1999, AIAA Paper 1999-0206.

[6]Chehroudi, B., Talley, D., and Coy, E., "Visual characteristics and initial growth of round cryogenic jets at subcritical and supercritical pressures," *Physics of Fluids*, Vol. 2, 2002, pp. 850–861.

[7]Leyva, I., Chehrodi, B., and Talley, D., "Dark core analysis of coaxial injectors at sub-, near-, and supercritical pressures in a transverse acoustic field," *43rd AIAA Joint Propulsion Conference*, Cincinnati, OH, July 2007.

[8]Roy, A., Joly, C., and Segal, C., "Disintegrating supercritical jets in subcritical environments," *Journal of Fluid Mechanics*, Vol. 717, 2013, pp. 193–202.

[9]Okong'o, N. and Bellan, J., "Direct numerical simulation of a transitional supercritical binary mixing layer: heptane and nitrogen," *Journal of Fluid Mechanics*, Vol. 464, 2002, pp. 1–34.

[10]Masi, E., Bellan, J., Harstad, K., and Okong'o, N., "Multi-species turbulent mixing under supercritical-pressure conditions: modeling, direct numerical simulation and anlysis revealing species spinodal decomposition," *Journal of Fluid Mechanics*, Vol. 721, 2013, pp. 578–626.

[11]Bellan, J., "Supercritical (and subcritical) fluid behavior and modeling: drops, streams, shear and mixing layers, jets and sprays," *Progress in Energy and Combustion Science*, Vol. 26, 2000, pp. 329–366.

[12]Oefelein, J., "Mixing and combustion of cryogenic oxygen-hydrogen shear coaxial jet flames at supercritical pressure," *Combustion Science and Technoligy*, Vol. 178, 2006, pp. 229–252.

[13]Dahms, R. and Oefelein, J., "On the transition between two-phase and single-phase interface dynamics in multicomponent fluids at supercritical pressures," *Physics of Fluids*, Vol. 25, 2013, pp. 1–24.

[14]Poling, B., Prausnitz, J., and O'Connell, J., *The Properties of Liquids and Gases*, McGraw-Hill, New York, fifth edition ed., 2001.

[15]Walas, S., *Phase Equilibria in Chemical Engineering*, Butterworth Publishers, Boston, 1985.